




Original Article



Plasma Extracellular Vesicle-derived MicroRNA Associated with Human Alpha-1 Antitrypsin Deficiency-mediated Liver Disease

Regina Oshins¹, Zhiguang Huo², Zachary Greenberg³, Virginia Clark⁴, Sergio Duarte⁵, Huiping Zhou⁶, Jesse West¹, Mei He³, Mark Brantly¹ and Nazli Khodayari^{1*} 

¹Department of Medicine, Division of Pulmonary, Critical Care and Sleep Medicine, University of Florida, Gainesville, FL, USA; ²Department of Biostatistics, College of Public Health, University of Florida, Gainesville, FL, USA; ³Department of Pharmaceutics, College of Pharmacy, University of Florida, Gainesville, FL, USA; ⁴Department of Medicine, Division of Gastroenterology, Hepatology, and Nutrition, University of Florida, Gainesville, FL, USA; ⁵Department of Surgery, Division of Transplantation and Hepatobiliary Surgery, University of Florida, Gainesville, FL, USA; ⁶Department of Microbiology and Immunology, Virginia Commonwealth University, Richmond VA Medical Center, Richmond, VA, USA

Received: July 25, 2024 | Revised: September 30, 2024 | Accepted: November 04, 2024 | Published online: November 19, 2024

Abstract

Background and Aims: Alpha-1 antitrypsin deficiency (AATD) is a genetic disorder associated with liver disease, ranging from fibrosis to hepatocellular carcinoma. The disease remains asymptomatic until its final stages when liver transplantation is the only available therapy. Biomarkers offer an advantage for disease evaluation. The presence of microRNAs (miRNAs) in plasma extracellular vesicles (EVs) presents a noninvasive approach to assess the molecular signatures of the disease. In this study, we aimed to identify miRNA biomarkers to distinguish molecular signatures of the liver disease associated with AATD in AATD individuals. **Methods:** Using small RNA sequencing and qPCR, we examined plasma EV miRNAs in healthy controls (n = 20) and AATD patients (n = 17). We compared the EV miRNAs of AATD individuals with and without liver disease, developing an approach for detecting liver disease. A set of miRNAs identified in the AATD testing cohort was validated in a separate cohort of AATD patients (n = 45). **Results:** We identified differential expression of 178 EV miRNAs in the plasma of the AATD testing cohort compared to controls. We categorized AATD individuals into those with and without liver disease, identifying 39 differentially expressed miRNAs. Six miRNAs were selected to test their ability to discriminate liver disease in AATD. These were validated for their specificity and sensitivity in an independent cohort of 45 AATD individuals. Our logistic model established composite scores with three- and four-miRNA combinations, achieving areas under the curve of 0.737 and 0.751, respectively, for predicting AATD liver disease. **Conclusions:** We introduce plasma EV-derived miRNAs as potential biomarkers for evaluating AATD liver disease. Plasma EV-associated miRNAs may represent a mo-

lecular signature of AATD liver disease and could serve as valuable tools for its detection and monitoring.

Citation of this article: Oshins R, Huo Z, Greenberg Z, Clark V, Duarte S, Zhou H, *et al.* Plasma Extracellular Vesicle-derived MicroRNA Associated with Human Alpha-1 Antitrypsin Deficiency-mediated Liver Disease. *J Clin Transl Hepatol* 2024. doi: 10.14218/JCTH.2024.00253.

Introduction

Alpha-1 antitrypsin deficiency (AATD) is a rare genetic disorder with a high prevalence in northwestern Europe and North America.¹ AATD is caused by a single mutation in the *SERPINA1* gene, resulting in misfolding and polymerizing of the Z mutant form of alpha-1 antitrypsin (AAT) in hepatocytes, rather than its secretion.² AAT is the most abundant serine protease inhibitor in the plasma. While intrahepatic accumulation of misfolded AAT can lead to liver disease, the resultant low levels of AAT in the circulating plasma can cause lung inflammation in AATD patients.³ In adult AATD individuals, liver disease is often underdiagnosed until the final stage of cirrhosis, when liver transplantation is the only treatment option.⁴ In AATD children, some may present with jaundice or cirrhosis, also requiring liver transplantation.⁵

Liver fibrosis and cirrhosis are major causes of worldwide morbidity and mortality, with limited therapeutic options, often leading to hepatocellular carcinoma (HCC). While cirrhosis is irreversible, new evidence indicates that liver fibrosis is dynamic and reversible.⁶ Liver fibrosis in AATD patients is primarily caused by hepatotoxicity due to the abnormal accumulation of AAT in hepatocytes.⁷ It is crucial to assess the extent of the hepatic AAT burden and identify individuals in the early stages of the disease to implement curative treatments before cirrhosis develops. Currently, liver biopsy is the gold standard for diagnosing AATD-mediated liver disease and assessing the stage of fibrosis.⁷ However, the biopsy is an invasive procedure associated with various complications.

Keywords: Alpha-1 antitrypsin; Liver disease; Fibrosis; Inflammation; Extracellular vesicles; MicroRNA; Biomarker; Molecular signature.

*Correspondence to: Nazli Khodayari, Department of Medicine, Division of Pulmonary, Critical Care and Sleep Medicine, University of Florida, 1345 Center Drive, Gainesville, FL 32610, USA. ORCID: <https://orcid.org/0000-0002-4659-1622>. Tel: +1-3522945198, E-mail: nazli.khodayari@medicine.ufl.edu.

Table 1. Demographics of study subjects

	MM (n = 20)	ZZ PASD 0–1 (n = 24)	ZZ PASD 2–3 (n = 38)
Age (years)	52 (37–79)	55 (25–71)	58 (40–70)
Sex (Female%)	60	71	47
Augmentation (%)	N/A	58	60
FEV1 (%)	N/A	67.3	61.2
ALT (U/L)	N/A	22.7	24.0
AST (IU/L)	N/A	29.7	29.1

MM, non-AATD individuals; ZZ, AATD individuals; PASD, Periodic Acid-Schiff positive Diastase-resistant stain; FEV1, Forced expiratory volume in one second; ALT, Alanine aminotransferase; AST, Aspartate aminotransferase.

Additionally, the limited size of liver samples and the subjective nature of pathological assessment limit the accuracy and reproducibility of histologic diagnoses.⁸ Given these challenges, alternative approaches are needed to overcome the limitations of liver biopsy in diagnosing and assessing liver disease in AATD patients.

Extracellular vesicles (EVs), with diameters ranging from 30 to 200 nm, are released by all cells in the body.⁹ EVs selectively carry signaling biomolecules such as microRNAs (miRNAs), messenger RNAs, proteins, and lipids. Most biofluids, including plasma and serum, contain a significant number of EVs, which coordinate multiple physiological and pathological processes through cargo transfer between cells and organs.^{3,9} In the liver, almost all cells, including hepatocytes, release and receive EVs. EVs play an important role in the initiation and progression of liver diseases, including inflammatory disorders and fibrosis.⁹ The study of EV contents has emerged as a promising area for discovering new biomarkers in liver disease.⁹

MiRNAs are commonly associated with EVs,¹⁰ and several EV-associated miRNAs have been found to be altered and linked to different types of liver diseases.^{11,12} These miRNAs have been shown to be associated with the clinical stage of various liver diseases, such as metabolic chronic liver disease and viral hepatitis.¹¹ AATD-mediated liver disease is characterized by a toxic “gain-of-function” mechanism involving ER and oxidative stress, mitochondrial dysfunction, and lipotoxicity.⁷ However, there has been no systematic screening of plasma EV-associated miRNAs for hepatotoxic features of AATD. Additionally, there is no consensus on the potential use of circulating miRNAs as diagnostic indicators for detecting AATD-associated liver disease.

In this study, we employed an innovative approach to compare miRNA profiles of plasma-derived EVs from AATD individuals with and without liver disease, as compared with non-AATD healthy controls. We chose to focus specifically on EV-associated miRNAs rather than free-circulating miRNAs in plasma for several reasons. While free miRNAs may originate from non-specific sources, such as general cell death or injury, EV-associated miRNAs have higher stability, a more targeted role in cell-to-cell communication, are more disease-specific, and have reduced background noise in plasma, thereby increasing the likelihood of identifying disease-specific biomarkers.¹³ The current gold standard for diagnosing AATD involves measuring serum AAT levels, followed by genotyping to identify mutations in the SERPINA1 gene. It is important to note that our objective was not to identify miRNA biomarkers to distinguish AATD individuals from non-AATD subjects. Instead, our integrative approach involved analyzing both AATD individuals and non-AATD healthy controls, followed by filtering steps to identify miR-

NAs that could provide insights into AATD liver disease status and aid in detecting AATD individuals at risk of developing pathological liver disease. Although they are not yet part of the standard diagnostic process, EV miRNAs could serve as molecular markers for early detection, monitoring liver disease progression, or assessing treatment response in AATD patients. However, further validation and large-scale studies are needed before EV miRNAs can be integrated into routine clinical practice.

Methods

Human subjects

The study protocol was approved by the Clinical Research Ethics Committee of the University of Florida (IRB202101148), and written informed consent was obtained from all subjects in accordance with the Declaration of Helsinki Principles.¹⁴ AATD individuals (n = 62; ages 35–70 years; mean 59 years; male:female ratio 9:10) were recruited by pulmonologists specialized in AATD at the University of Florida Shands Hospital (n = 17 in the testing cohort and n = 45 in the validation cohort). Diagnosis of AATD was established by genotyping, isoelectric focusing of serum proteins, and measurement of AAT serum levels by nephelometry (Behring Diagnostics, Marburg, Germany) using in-house standards and controls.¹⁵ Percutaneous liver biopsy was performed on a well-characterized cross-section of adults with AATD, as previously reported.⁷ A group of age- and gender-matched non-AATD control individuals (n = 20; ages 37–79 years; mean 52 years; male: female 2: 3) from the Alpha-1 Foundation DNA and Tissue Bank were also recruited. Detailed clinical data of subjects enrolled in this study are shown in Table 1.

Sample collection and processing

Blood samples were collected from participants following guidelines set by the International Society for Extracellular Vesicles.¹⁶ The collected blood was centrifuged at 2,500xg for 10 m at room temperature, and plasma was separated, aliquoted, and stored at –80°C. Plasma aliquots were thawed on ice, quickly swirled in a 37°C water bath until clear, and then centrifuged for 5 m at 18,000xg at 4°C. The supernatant was removed and passed through a 0.8 mm filter prior to EV extraction. Four milliliters of plasma were used per sample.

EV isolation

EVs were isolated from cryopreserved plasma using differential centrifugation, as described previously.³ Briefly, plasma samples were ultracentrifuged in a Beckman Coulter Optima XE90 Ultracentrifuge with an SW-40Ti swinging rotor at 110,000xg for 2 h at 4°C. EV pellets were resuspended

in PBS, filtered through a 0.22 µm filter (Millipore, Billerica, MA), and centrifuged at 110,000xg for 70 m at 4°C. The EVs were then resuspended in 200 µL of PBS and stored for further analysis.

RNase and proteinase treatment of isolated plasma EVs

Free RNA and proteins were removed from the isolated EV fractions by treatment with 100 µg/mL of Proteinase K (Qiagen, Hilden, Germany) for 30 m at 37°C, followed by 10 µg/mL of RNase A (Qiagen, Hilden, Germany) for 15 m at 37°C.

EV protein quantification

Protein concentrations of EV fractions were quantified using the Pierce BCA Protein Assay Kit (Thermo Scientific, Waltham, MA) according to the manufacturer's instructions. Four microliters of each standard and lysed EV sample were mixed into a 96-well plate with 200 µL of reaction buffer. The plate was incubated at 37°C for 30 m, and absorbance at 562 nm was measured using a spectrophotometer (SpectraMax, Molecular Devices). A standard curve was used to determine the protein concentration.

EV characterization

Purified EVs were characterized for size, concentration, presence of specific EV markers, and morphology. To assess morphology and size, isolated EVs were subjected to transmission electron microscopy and nanoparticle tracking analysis (NTA), as previously described.³ EVs were also analyzed for the presence of CD81, CD63, and TSG101 as specific EV markers and for the absence of the ER marker Calnexin by western blot analysis.

RNA isolation and library preparation

RNA from EV fractions was isolated using the exoRNeasy Maxi Kit (Qiagen, Germantown, MD), and the quantity and quality of RNA and small RNA were determined using the Agilent RNA 6000 Pico Kit and Small RNA Kit on the Agilent Bioanalyzer, following the manufacturer's instructions. Sequencing libraries were constructed using approximately 6 ng of total EV-derived RNA with the Small RNA Library Prep Set for Illumina (New England Biolabs), according to the manufacturer's protocol. Each adapter-ligated RNA was mixed with ProtoScript II reverse transcriptase, RNase Inhibitor, and first-strand synthesis reaction buffer (NEB, catalog number E7560S) and incubated for 60 m at 50°C. Index codes were added to each reaction product for sample differentiation. Size selection was performed using a 6% polyacrylamide gel. For miRNA, bands corresponding to ~150 bp were isolated. Library quality was assessed with the Agilent Bioanalyzer 2100 and Qubit, and libraries were sequenced using the Illumina MiSeq 1 × 150 cycles V3 kit at the University of Florida Interdisciplinary Center for Biotechnology Research.

Mice and treatments

The study protocol was approved by the ethics committee of the University of Florida (IACUC 20230000056). Wildtype, C57/B6 mice, aged 12 weeks, were housed under controlled environmental conditions (12-h light/dark cycle; temperature 22–24°C) and provided food and water ad libitum in the Animal Care Facility. Mice were divided into three groups: Group 1 (n = 6) consisted of control animals injected intraperitoneally with CCl₄ (Sigma-Aldrich, St. Louis, MO, USA) (0.3% CCl₄, 10 µL/g of body weight, twice weekly) for four weeks to induce liver fibrosis. Groups 2 and 3 (n = 6/group) were injected intraperitoneally with CCl₄ using the same

schedule and dosing as Group 1, along with intravenous injections of EVs derived from either normal or AATD plasma (1 × 10⁹ EVs, pooled from three subjects, twice weekly). All animals were euthanized 48 h after the last dose of CCl₄, and their livers were collected for analysis.

Small RNA-sequencing and bioinformatics

After removing adapters using cutadapt software,¹⁷ the small RNA sequencing reads were aligned to the Genome Reference Consortium Human Build 38 (hereinafter referred to as GRCh38) using bowtie2 software¹⁸ with “-very-sensitive-local” option for local alignment, which does not require reads to align end-to-end. miRNA expression count data were extracted using HTSeq software^{19,20} with the miRBase Sequence Database (release 22)²¹ as the gene annotation reference. The resulting miRNA expression data were further normalized using the count per million reads method, followed by log₂(x+1) transformation, where x is the expression value and 1 is the pseudo count. Low-quality sequences were trimmed, and poor-quality reads were removed using Trimmomatic.²² Star Aligner was used to map high-quality paired-end reads to the human genome (GRCh38).²³ Gene expression was obtained using RSEM.²⁴

Functional pathway and network analyses

We performed pathway enrichment analysis using Ingenuity Pathway Analysis (IPA) (Ingenuity Systems, Inc., Redwood, CA). IPA core analyses are based on previous knowledge of associations within causal networks and their downstream target genes archived in the Ingenuity knowledge base.²⁵ An overlap *p*-value, based on the significant overlap between networks and their targets, and an activation *z*-score were computed. The activation *z*-score is used to infer likely activation or inhibition states of causal networks. Networks were considered significantly activated or inhibited if the overlap *p*-value was ≤0.05 and the *z*-score was ≤2.0 (or ≥-2.0).

Bibliographic search and miRNA selection

A literature search of PubMed and the Liver Disease Micro-RNA Signature²⁶ databases was conducted to identify dysregulated miRNAs in various liver diseases. We combined this bibliographic information with our results from next-generation sequencing (NGS) of plasma-derived EVs from AATD and healthy control samples. A group of highly expressed miRNAs (each producing over 5,000 reads in the NGS assay and belonging to the most abundant miRNAs identified by NGS) were further considered for biomarker studies as molecular identifiers for the severity of AATD-associated liver disease.

Real-time qPCR validation of selected miRNAs

Reverse transcription reactions were performed using TaqMan Advanced miRNA Assays (Applied Biosystems Inc., CA) with 2 µL of cell-free RNA extracted from plasma-derived EVs to prepare cDNA. Real-time PCR reactions were performed in duplicate on an Applied Biosystems 7500 Fast thermocycler, programmed as follows: 95°C for 20 s, followed by 40 cycles of 95°C for 1 s and 60°C for 20 s. We used hsa-miR-21-5p and hsa-miR-26a-5p, two of the most stable miRNAs in terms of read counts, as endogenous controls. All fold-change data were obtained using the 2^{-ΔΔCt} method.²⁷

Liver histology

Percutaneous liver biopsy on AATD individuals was performed with a 16-gauge BioPince™ core biopsy needle. The samples were formalin-fixed and processed for further examination. Hematoxylin & Eosin (H&E), Masson's Trichrome, and Period-

ic Acid-Schiff positive, Diastase-resistant (PASD) stains were performed on the liver sections. Two pathologists scored each biopsy for fibrosis using METAVIR stages F0–F4 based on Masson's Trichrome staining. Clinically significant fibrosis was defined as stage \geq F2. PASD staining was also used to identify AAT accumulation and assess AATD-mediated liver disease severity. PASD globules present in a high-power field were scored from 0–3 as follows: 0 - None, 1 - Rare ($<$ 5 hepatocytes with globules), 2 - Few (5–20 hepatocytes with globules), 3 - Numerous (\geq 20 hepatocytes with globules).⁷ Mouse liver tissues were also formalin-fixed and stained for collagen deposition (Picrosirius Red) or α -smooth muscle actin as an indication of hepatic stellate cell activation.

Statistical analysis

After removing non-expressed miRNAs, differential analysis was performed using the edgeR package,²⁸ which employs a negative binomial distribution to model count data. For RNA-Seq data, we performed differential expression analysis using edgeR.^{27,28} Thresholds were set at a false discovery rate (q -value) \leq 0.05 and a log₂ fold change of $>$ 1 or $<$ -1 (linear fold change of \geq 2). Each miRNA's predictive power was determined by a receiver operating characteristic (ROC) curve. To ensure accurate and reliable ROC analysis, miRNA data were normalized by count per million reads, log₂-transformed, and standardized. In the ROC curve, PASD status (no liver disease [PASD 0–1] vs. liver disease [PASD 2–3]) was the outcome variable, and the expression level of each miRNA was the predictor. By varying miRNA expression criteria in the prediction of PASD status, we obtained a series of prediction sensitivities and specificities. The optimum sensitivity and specificity were chosen such that the Youden index was maximized, where the Youden index = sensitivity + specificity - 1. To assess over-predictive power, we calculated the area under the curve (AUC). An AUC of one indicates perfect prediction, while an AUC of 0.5 is equivalent to random guessing. To explore the combined predictive power of miRNA panels (e.g., sets of three or four miRNAs), we constructed composite scores using logistic regression and assessed their performance using ROC analysis. To ensure validity and avoid overfitting, we tested these composite scores on an independent cohort of 45 AATD cases.

Results

Isolation and characterization of EV

EVs were isolated from the plasma of 20 non-AATD control subjects (MM) and 62 AATD individuals (ZZ) with different stages of liver disease using a combination of filtration and ultracentrifugation. EV fractions were fully characterized by analyses of particle size, distribution, and concentration.³ NTA was performed to assess size distribution and concentration of EVs in both AATD patients and control groups. Figure 1A presents the average particle size profiles for each group, with no significant differences in size distribution between samples. EV isolated from the plasma of both MM and ZZ groups were within the normal range for EV size (below 150nm), and the EV recovery in ZZ individuals was the same as in the MM control group (Fig. 1A). No AUC analysis was conducted, as NTA is designed to measure particle size and concentration, rather than providing data suitable for AUC comparison. The cup-shaped morphology of the EVs was confirmed in both MM (top) and ZZ individuals (bottom) by transmission electron microscopy (Fig. 1B). Results from western blot analysis confirmed the expression of CD63, CD81, and TSG101 EV markers in all EV fractions,

while Calnexin (EV negative control marker) was not detected (Fig. 1C). Coomassie blue staining showed that Proteinase K treatment degraded most proteins in both plasma and the isolated EV fraction (Fig. 1D). After Proteinase K and RNase treatment, we observed that EV isolated from the plasma of the MM group had slightly higher concentrations (p -value $<$ 0.05) of total RNA compared to EV isolated from the plasma of the ZZ group (Fig. 1E).

Plasma EV-derived miRNA profile of AATD and control individuals and validation of miRNAs by RT-qPCR

To obtain the profile of plasma EV-derived miRNA in AATD individuals and non-AATD controls, we first analyzed 37 plasma EV samples (17 AATD, 20 non-AATD controls) by small RNA sequencing. Based on raw data, an average of 6,116,653 raw reads per sample were obtained for non-AATD control samples and 11,846,649 reads per sample for the AATD group (Supplementary Table 1), reflecting a significant difference between the two groups (p -value $<$ 0.001). A total of 682 mature known miRNAs were identified among all samples. More than 80% of these miRNAs (574 miRNAs) were already included in the vesicular database Vesiclepedia, and 36% (246 miRNAs) were included in EVpedia as related to EVs from human samples (Fig. 2A). The complete list of identified miRNAs has been submitted to the EVpedia database under the title of this manuscript. In differential expression analysis ($|\log_2(\text{F.C.})| >$ 1, q -value $<$ 0.05), 178 miRNAs were found to be differentially expressed between AATD individuals (regardless of whether they had liver disease) and non-AATD healthy controls. Out of these 178 differentially expressed miRNAs (DEMs), 92 miRNAs were upregulated, and 86 miRNAs were downregulated in AATD individuals compared to healthy controls (Fig. 2B and C). Our small RNA-seq data indicated that miR-25-3p, miR-99b-3p, and miR-30a-5p were highly upregulated, while miR-451a, miR-374a-5p, miR-146a-5p, miR-16-5p, miR-26b-5p, miR-96-5p, and miR-142-5p were highly downregulated in the plasma EVs of AATD individuals compared to non-AATD healthy controls (Supplementary Fig. 1A). To validate these small RNA sequencing results, 20 miRNAs were randomly chosen from the 178 DEMs to ensure an unbiased validation of our findings. This approach allowed us to confirm the reproducibility and reliability of the sequencing results across a diverse set of miRNAs. Relative expressions of these miRNAs were determined by RT-qPCR measurements using hsa-miR-26a-5p as a reference.²⁹ Expression of hsa-miR-125a, hsa-miR-128-3p, hsa-miR-99a-5p, hsa-miR-335-5p, hsa-miR-361-3p, hsa-miR-150-5p, hsa-miR-30e-5p, hsa-miR-193a-5p, and hsa-miR-23a-3p were significantly upregulated in AATD individuals (Supplementary Fig. 1B) compared to controls (Mann-Whitney p -values $<$ 0.001). Expression of hsa-miR-16-5p and hsa-miR-142-3p was significantly downregulated in AATD individuals (Supplementary Fig. 1C) compared with controls (Mann-Whitney p -values $<$ 0.001). We also observed that with a 95% confidence interval, the fold change values obtained from both methods overlapped in 10 cases (Fig. 2D). Moreover, fold change values obtained from these two different methods were highly correlated (Pearson's correlation 0.86, p -value 0.0013).

Correlation of plasma EV-miRNA with PASD and fibrosis scores in AATD individuals

As we have previously shown,⁷ AATD-mediated liver disease is characterized by hepatic accumulation of misfolded AAT, forming PASD globules in the hepatocytes (PASD scores 0–3), and subsequent liver fibrosis (METAVIR scores 0–3), as measured by Masson's Trichrome staining (Fig. 3A). In this study, we conducted two separate analyses to detect

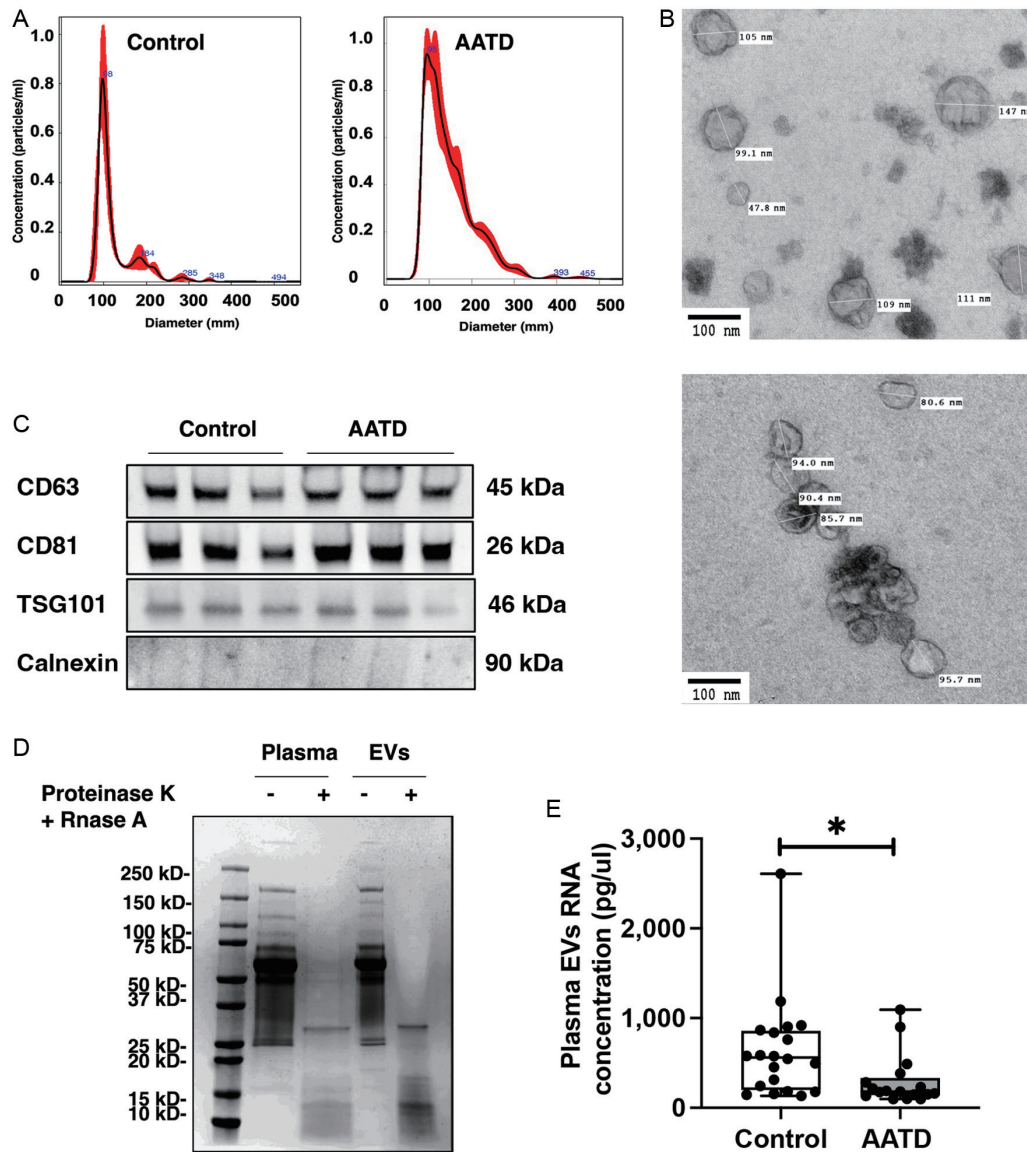


Fig. 1. Isolated EVs enriched fractions from participants' plasma. (A) Nano tracking analysis results suggested that EVs isolated from the plasma of control and AATD individuals (pooled from three individuals/group) were about 75–200 nm in diameter. (B) TEM images of EV fractions isolated from the plasma of control (top) and AATD individuals (bottom). (C) EV surface markers CD63, CD81, and TSG101 were all detected by western blot in the EV fractions of the plasma, while Calnexin, a negative marker for EVs, was absent in our isolated EV fraction samples. (D) Isolated EV fractions were treated with RNase A and protease K to eliminate the membrane-bound RNAs and proteins from EVs. (E) A box plot comparing the RNA concentration (pg/μl) of EV fractions isolated from control and AATD individuals. **p*-value < 0.05. EV, extracellular vesicle; AATD, alpha-1 antitrypsin deficiency.

correlations between EV-associated DEMs with (A) PASD, and (B) fibrosis scores in 17 AATD individuals, considering each individual's PASD and fibrosis scores, respectively. We identified 89 miRNAs whose expression increases with increasing PASD scores, and 68 miRNAs whose expression was associated with increasing fibrosis scores in these 17 AATD individuals. Notably, there was an overlap of 60 DEMs where expression was associated with both PASD and fibrosis scores (Fig. 3B). IPA target analysis revealed that these 60 DEMs, associated with both PASD and fibrosis scores, predominantly target genes such as Bcl2, Col1A1, Col4a, EGFR, FN1, and Pdgfr, and are involved in liver cell proliferation, activation, and fibrogenesis. The cord plot from ingenuity target analysis in Supplementary Figure 1D indi-

cates target genes that are involved in hepatic stellate cell activation, proliferation, and fibrogenesis. The 18 miRNAs displayed in the cord plot show the most relevant interactions with genes specifically linked to liver fibrogenesis. This result is consistent with our previous demonstration that the severity of fibrosis correlates with PASD scores in the liver of AATD individuals.⁷ To further investigate the impact of AATD circulating EVs and their miRNA content on hepatic stellate cell activation *in vivo*, we employed the established CCl₄ liver fibrosis model and administered either control or AATD plasma-derived EVs. After four weeks, mice treated with CCl₄ and AATD EVs exhibited a significant increase in α-smooth muscle actin-positive cells (activated hepatic stellate cells) within fibrotic septa and enhanced

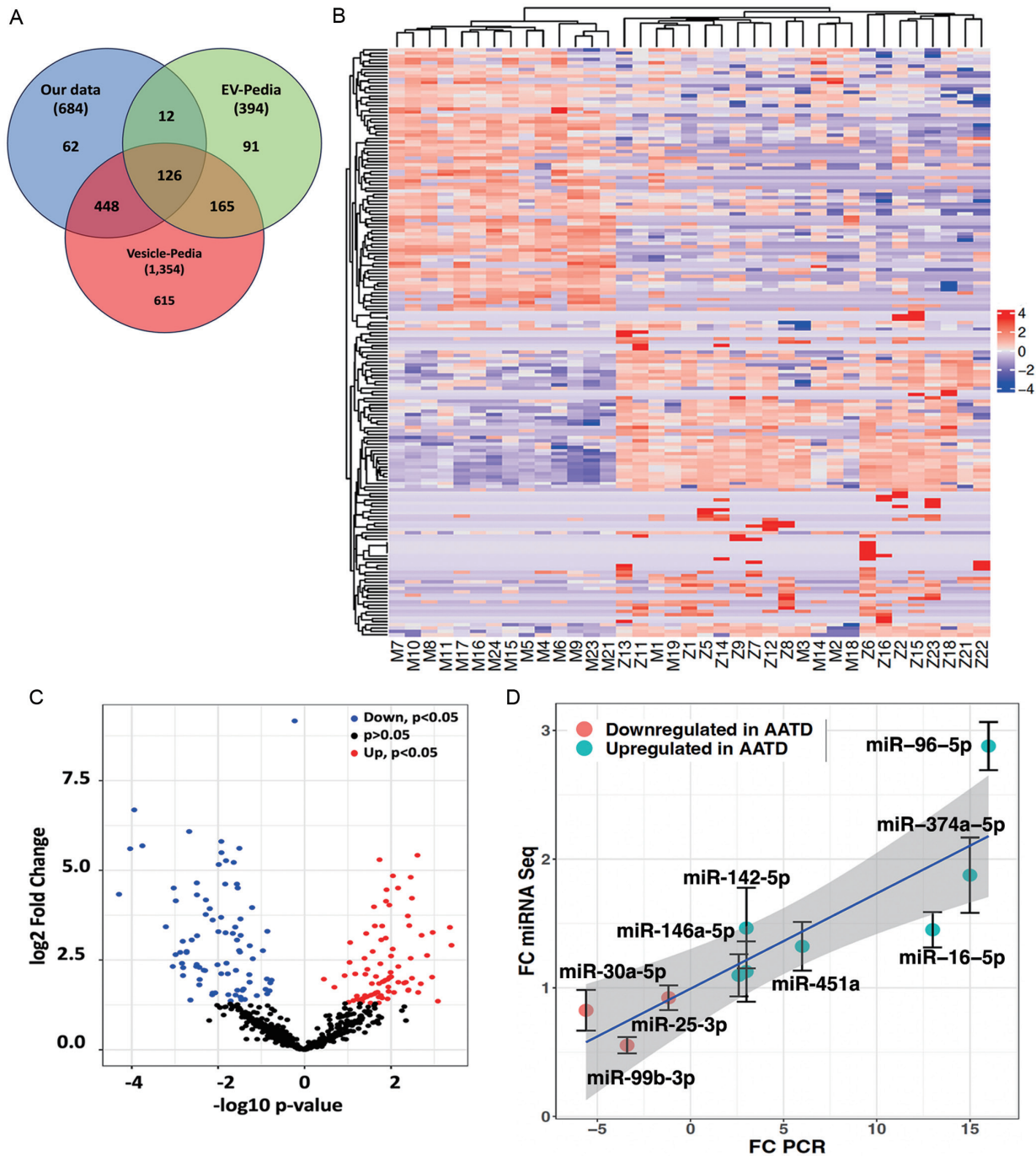


Fig. 2. Plasma EVs associated miRNA profile of AATD and control individuals. (A) Venn diagram showing DEMs shared between EVpedia and Vesiclepedia datasets and our plasma EV-derived miRNA dataset. (B) Heatmap and (C) Volcano plot of the 100 DEMs across 37 samples in our plasma EV-derived miRNA dataset. (D) The scatter plot highlights the high correlation found between small RNA-seq and qPCR methods (Pearson's correlation = 0.86, p-value = 0.0013). The solid line represents the linear regression of this correlation. EV, extracellular vesicle; AATD, alpha-1 antitrypsin deficiency; DEMs, differentially expressed miRNAs.

collagen deposition compared to those receiving CCl₄ with control EVs or CCl₄ alone (Fig. 3C).

Exploring potential plasma EV-associated miRNA biomarker candidates to assess the severity of liver disease in AATD

We first divided the experimental set of 17 AATD individuals

into two subgroups: those with no liver disease (PASD scores 0–1) and those with liver disease (PASD scores 2–3). Our DEM analysis ($|\log_2(\text{F.C.})| > 1, p < 0.05$) unveiled 39 differentially expressed miRNAs (Fig. 4A). We then individually screened these 39 DEMs for their performance as potential biomarkers of AATD-mediated liver disease by executing a ROC and AUC analysis and calculating their specificity and

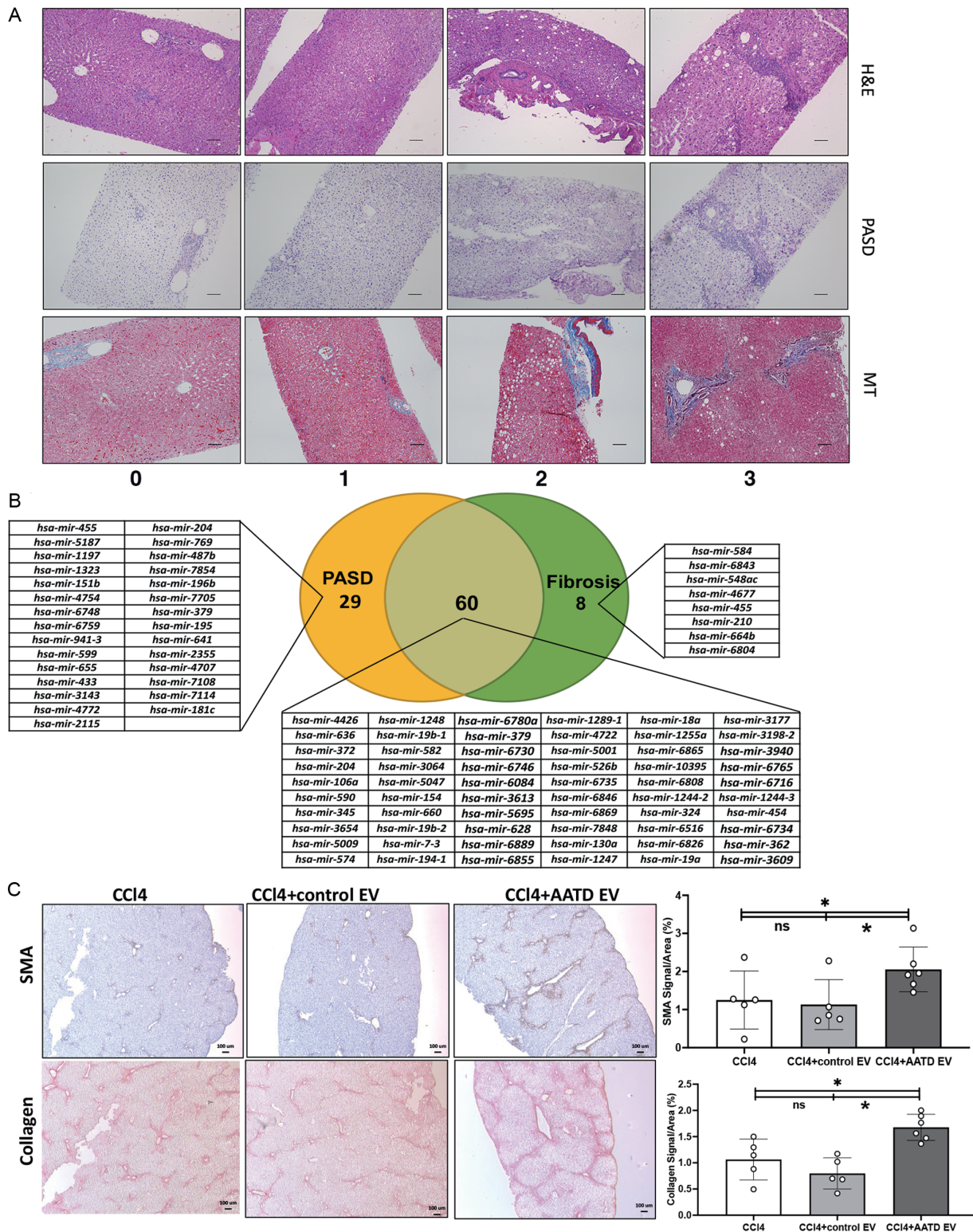


Fig. 3. Correlation of plasma EVs associated miRNA profile with PASD and fibrosis scores in AATD individuals. (A) Representative liver biopsies showing increasing fibrosis stages and PASD globule scores from AATD individuals. Top (H&E), middle (PASD), bottom (MT). Scale bar represents 200 μ m. (B) Associations between the differentially expressed EV-associated miRNAs and PASD and fibrosis scores in AATD individuals. (C) Significant increase in activated hepatic stellate cells, indicated by expression of α -SMA (top row), and collagen deposition in septa as determined by Picrosirius Red staining (bottom row) in the liver of mice treated with CCl₄ and AATD plasma EV, compared to mice treated with CCl₄ and control plasma EV. * $p < 0.05$, (n = 6). EV, extracellular vesicle; AATD, alpha-1 antitrypsin deficiency; PASD, alpha-1 antitrypsin globules; H&E, Hematoxylin & Eosin; MT, Masson's Trichrome; α -SMA, alpha-smooth muscle actin.

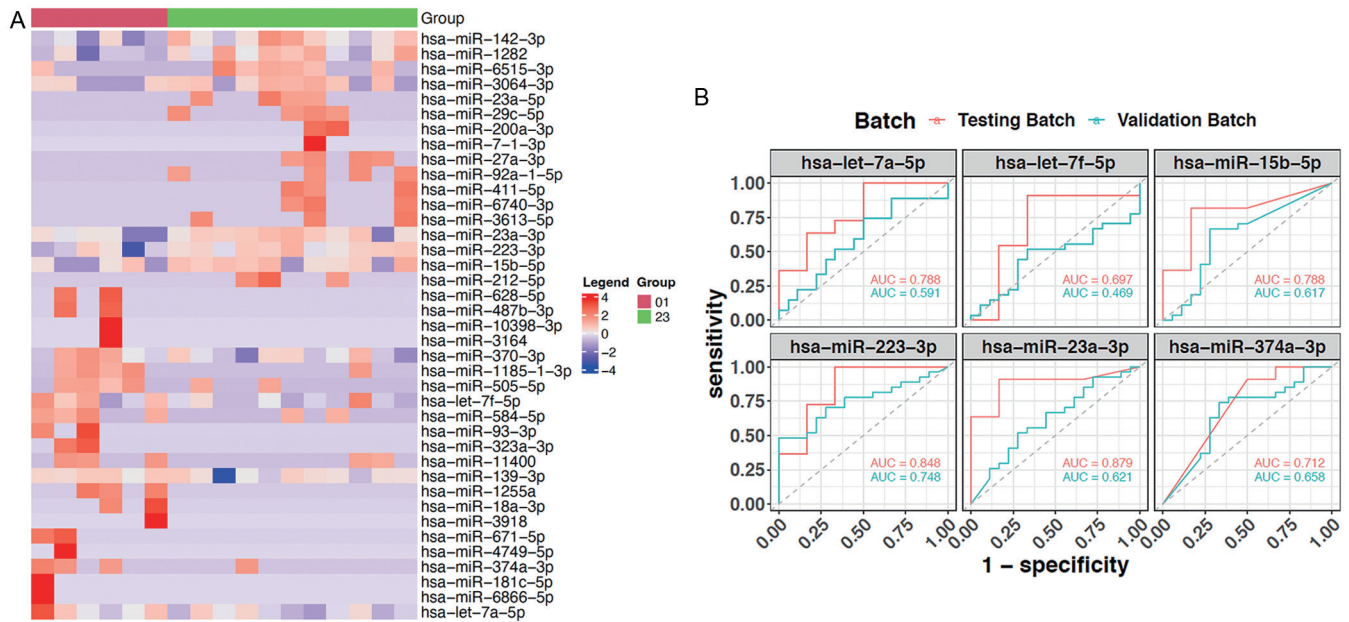


Fig. 4. Verification of EVs miRNA biomarker candidates for AATD liver disease severity. (A) Heatmap plot indicating 39 differentially expressed plasma EV-miRNAs across 17 AATD individuals (testing cohort) with and without liver disease. (B) Verification of EV-derived hsa-let-7a-5p, hsa-let-7f-5p, hsa-miR-15b-5p, hsa-miR-223-3p, hsa-miR-23a-3p, and hsa-miR-374a-3p as biomarkers of AATD-mediated liver disease. The ROC curves of the testing dataset (miRNA sequencing of 17 samples) are shown in red, while the ROC curves of the validation dataset (miRNA sequencing of 45 samples) are shown in turquoise. EV, extracellular vesicle; AATD, alpha-1 antitrypsin deficiency.

sensitivity. Most candidate DEMs (24 miRNAs) displayed a specificity of 0.7–1.0 and a sensitivity of 0.8–1.0 (Table 2). From these DEMs, a total of 6 miRNAs were selected based on significant differential expression, as well as theoretical evidence for clinical application in liver disease based on previous studies (Table 3).^{30–42} To validate the specificity of these six plasma EV-derived miRNAs for AATD individuals in the testing set, ROC analysis was performed, and AUC was calculated for each of these miRNAs in both the testing ($n = 17$) and validation ($n = 45$) cohorts of AATD individuals (total of 62 AATD patients) (Fig. 4B).

Diagnostic efficacy comparison of miRNA panel candidates in AATD-associated liver disease

To further verify miRNA combination panels for AATD-associated liver disease diagnosis, we performed a diagnostic performance analysis in our independent validation cohort containing 45 AATD individuals. To develop a classification method, we used Fisher's linear discriminant analysis and designed comprehensive classifiers consisting of three and four miRNAs in the training set (Supplementary Tables 2 and 3). The most significant results of the three-miRNA combinations are shown in Figure 5A (AUC = 0.73), and the results from four-miRNA combinations are demonstrated in Figure 5B (AUC = 0.75). The performance of miRNA panels in the testing cohort (AUC = 0.95–1) is higher for AATD-associated liver disease diagnosis than in the validation cohort.

Discussion

Here, we conducted a comprehensive analysis of plasma EV-associated miRNAs in AATD individuals, comparing them to non-AATD controls.⁴³ We also focused on comparing miRNA profiles from AATD individuals with and without liver disease. We identified 6 miRNAs as potential molecular identifiers for the detection of AATD liver disease. We suggest that pan-

els consisting of three and four miRNAs could offer potential biomarkers for assessing the severity of AATD liver disease.

Our results revealed that among the DEMs associated with AATD, miR-25-3p, miR-96-5p, and miR-30a-5p have been previously reported as HCC biomarkers.^{44–51} Consistent with previous literature, our results also suggest that AATD liver disease is a risk factor for HCC.⁷ This suggests that plasma EV-associated miRNAs can serve as molecular signatures of HCC in AATD individuals. Studies have shown high extracellular levels of miR-99-3p,⁵² and low levels of miR-16⁵³ are linked to hepatic fibrosis. Given that liver fibrosis is found in 35% of AATD individuals,⁷ changes observed in AATD plasma EVs may represent a liver fibrosis diagnostic option in these patients. Furthermore, our *in vivo* experiments showed that plasma EVs derived from AATD patients enhanced CCl₄-induced liver fibrogenesis compared to control EVs, supporting the idea that AATD EVs may contribute to the promotion of fibrosis. This suggests that the miRNAs carried within these EVs likely play a role in liver disease progression by influencing fibrogenesis.

Network analysis of plasma EV-associated DEMs in AATD suggested an increase in the activity of different causal networks, including FOXP3, which is essential for immune cell function. Activated hepatic stellate cells in the fibrotic liver induce naive T cells to differentiate into Foxp3(+) cells.⁵⁴ While activation of hepatic stellate cells is the hallmark of liver fibrosis,⁵⁵ this finding suggests that FOXP3 activation may be downstream of hepatic stellate cell activation in the AATD liver. IPA also predicted inhibition of integrin $\beta 4$ (ITGB4) in the plasma EVs of AATD individuals (Supplementary Fig. 2A). While ITGB4 can promote liver fibrogenesis,⁵⁶ inhibition of ITGB4 may be a compensatory mechanism against AATD liver fibrosis.

AATD patients with positive liver PASD scores and liver fibrosis show an important pathological overlap, hampering correct diagnosis and management.⁷ The overlapping miRNA

Table 2. Top 24 miRNAs ranked by sensitivity specificity (miRNA-seq data)

miRNA_ID	log2FC	p-value	Sensitivity	Specificity	Sen x Spe
hsa-miR-30a-5p	1.73	5.05E-06	1	0.9	0.9
hsa-miR-10b-5p	2.42	0.00034	1	0.9	0.9
hsa-miR-361-3p	1.17	0.0077	0.88	1	0.88
hsa-miR-10a-5p	2.16	3.12E-05	1	0.85	0.85
hsa-miR-186-5p	-2.19	0.000117	1	0.85	0.85
hsa-let-7c-5p	1.79	0.000356	1	0.85	0.85
hsa-miR-451a	-3.94	2.08E-07	0.94	0.9	0.85
hsa-miR-223-3p	1.89	3.48E-05	0.94	0.9	0.85
hsa-miR-3615	2.48	5.99E-05	0.94	0.9	0.85
hsa-miR-20a-5p	-2.28	6.69E-05	0.94	0.9	0.85
hsa-miR-146a-5p	-1.92	1.57E-06	1	0.8	0.8
hsa-miR-96-5p	-4.03	2.50E-06	0.94	0.85	0.8
hsa-miR-30a-3p	2.04	1.42E-05	0.94	0.85	0.8
hsa-miR-28-3p	1.61	0.000104	1	0.8	0.8
hsa-miR-125a-5p	1.99	0.006954	0.94	0.85	0.8
hsa-miR-99b-5p	1.43	0.000576	0.82	0.95	0.78
hsa-miR-99a-5p	1.77	0.000865	0.94	0.8	0.75
hsa-miR-1244	1.45	0.00574	0.94	0.8	0.75
hsa-miR-16-5p	-3.75	2.07E-06	0.88	0.85	0.75
hsa-miR-194-5p	-2.49	4.83E-05	0.88	0.85	0.75
hsa-miR-370-3p	1.88	0.000773	0.88	0.85	0.75
hsa-miR-150-5p	2.04	0.00156	0.88	0.85	0.75
hsa-miR-139-5p	1.58	0.00182	1	0.75	0.75
hsa-miR-93-5p	-1.59	0.00613	1	0.75	0.75

signatures in our dataset suggest that PASD and fibrosis phenotypes share the same miRNA profiles, which points to a common injury process within the AATD liver. Our data also suggest common molecular pathways that may be relevant to other chronic liver diseases. This expands the potential clinical application of these biomarkers beyond AATD, opening possibilities for their use in other liver conditions. Among these overlapping miRNAs, we observed that the hsa-let-7 family represents 48% of miRNAs identified (Fig. 2B). While let-7a-5p was predicted to negatively correlate with collagen expression, previous studies have shown the inhibitory role of let-7a in liver fibrogenesis.⁵⁷ This suggests that the upregulation of let-7a-5p may be an anti-fibrotic defense mecha-

nism in the AATD liver. In terms of translational research, the identified miRNAs provide important mechanistic insights into AATD-related liver disease. For example, miR-23a-3p, associated with endoplasmic reticulum stress,⁵⁸ mitochondrial dysfunction,⁵⁹ and lipid accumulation,⁶⁰ offers new avenues for understanding the pathophysiology of AATD liver disease. These mechanistic insights could be harnessed to develop targeted therapies aimed at addressing the underlying causes of liver injury in AATD.

Conclusions

Here, we show unique properties of six plasma EV-associated

Table 3. Circulating plasma miRNAs related to liver diseases

miRNA_ID	Reported in patients' plasma (Ref)	Reported in liver disease (Ref)
hsa-let-7a-5p	Chronic Hepatitis C ³¹	Hepatic Fibrosis ³²
hsa-let-7f-5p	Hepatocellular Carcinoma ³³	Hepatocellular Carcinoma ³⁴
hsa-miR-15-5p	Hepatocellular Carcinoma ³⁵	Liver Cancer ³⁶
hsa-miR-233-3p	Acute-on-chronic liver failure ³⁷	Hepatocellular Carcinoma ³⁸
hsa-miR-23a-3p	NAFLD ³⁹	NAFLD ⁴⁰
hsa-miR-374a-3p	HBV-Liver fibrosis ⁴¹	Hepatitis B-related acute-on-chronic liver failure ⁴²

NAFLD, non-alcoholic fatty liver disease; HBV, hepatitis B virus.

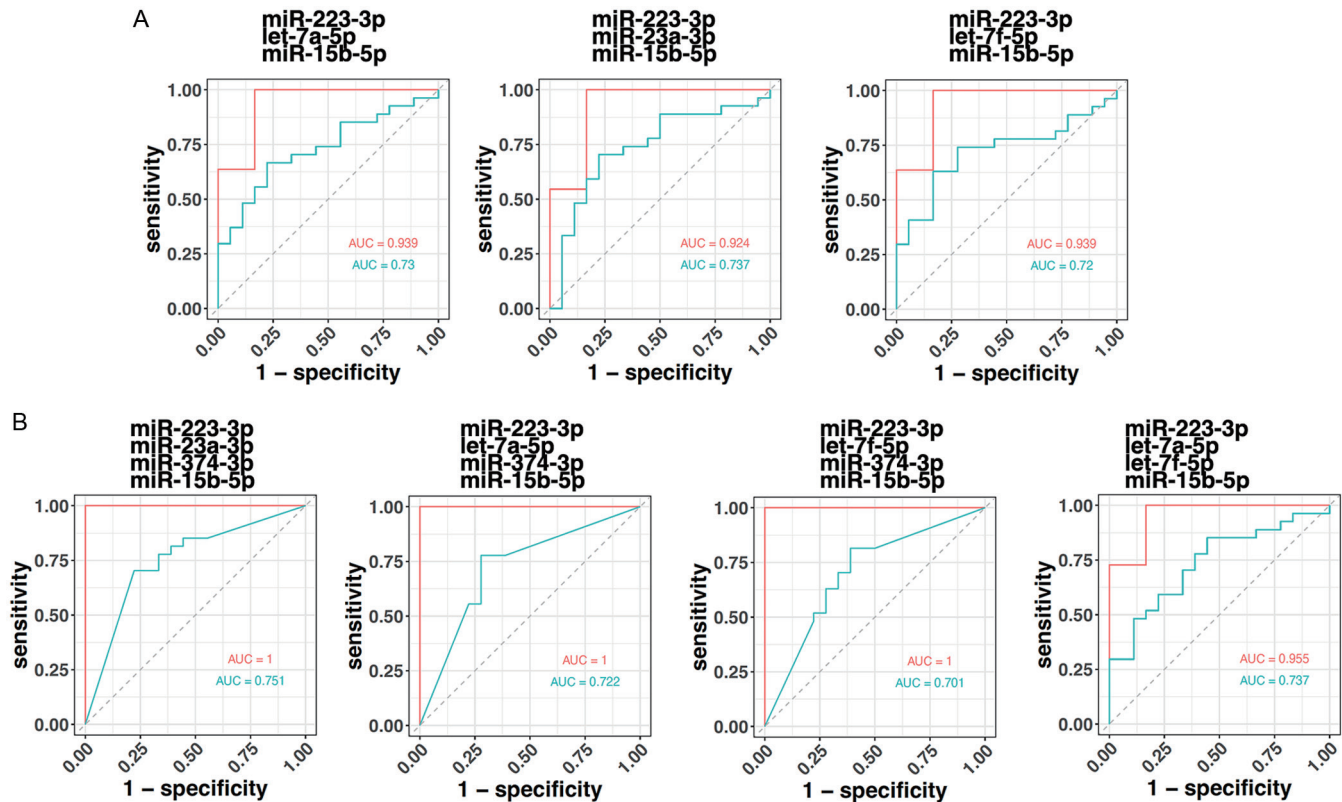


Fig. 5. Identification of EVs miRNA biomarker panel candidates for AATD liver disease severity. (A) Verification of three miRNA panels: panel 1 (miR-223-3p + let-7a-5p + miR-15b-5p), panel 2 (miR-223-3p + miR-32a-3p + miR-15b-5p), and panel 3 (miR-23a-3p + let-7f-5p + miR-15b-5p) as biomarkers of AATD-mediated liver disease. (B) Verification of four miRNA panels: panel 1 (miR-223-3p + miR-23a-3p + miR-374-3p + miR-15b-5p), panel 2 (miR-223-3p + let-7a-5p + miR-374-3p + miR-15b-5p), panel 3 (miR-223-3p + let-7f-5p + miR-374-3p + miR-15b-5p), and panel 4 (miR-223-3p + let-7a-5p + let-7f-5p + miR-15b-5p) as biomarkers of AATD-mediated liver disease. The ROC curves of the testing dataset (miRNA sequencing of 17 samples) are shown in red, while the ROC curves of the validation dataset (miRNA sequencing of 45 samples) are shown in turquoise. EV, extracellular vesicle; AATD, alpha-1 antitrypsin deficiency.

miRNAs, and their combinations offer a valuable tool for early detection and risk stratification. With high diagnostic accuracy (AUC > 0.93 in training batches and AUC > 0.75 in validation batches), our designed panels may enable clinicians to detect liver disease in AATD patients early and potentially intervene before severe complications, such as cirrhosis or HCC. The use of these miRNAs as non-invasive disease signatures is especially advantageous for patients, as it reduces the need for invasive liver biopsies. This facilitates regular monitoring of liver health in AATD individuals, particularly those who may not yet show clinical symptoms of liver disease. Our results have significant clinical and translational implications, particularly in improving the detection and management of liver disease in AATD individuals. Moreover, the study suggests that these miRNA panels could be used to monitor therapeutic responses to anti-fibrotic treatments. This could accelerate the development of new therapies by providing a quicker and less invasive way to assess treatment efficacy in clinical trials.

Finally, this study contributes to the growing field of precision medicine by identifying miRNA signatures that can help predict disease severity and progression in AATD patients. These disease molecular signatures could facilitate personalized treatment plans based on individual risk profiles, improving patient outcomes and reducing unnecessary interventions for those with a lower likelihood of developing advanced liver disease.

While our findings point to the potential use of plasma EV

miRNAs as molecular identifiers for liver disease in AATD individuals, it's important to note that further research on plasma-derived free miRNAs is needed to confirm the effectiveness of plasma EV-associated miRNAs. We acknowledge that our study has several limitations, such as the small number of individuals included, which may impact the robustness of our model. However, it is important to emphasize that AATD is a rare condition, with a frequency of approximately one in 1,800 individuals, presenting significant challenges in terms of participant recruitment. Many AATD individuals remain undiagnosed or misdiagnosed, as the condition can mimic more common respiratory diseases like COPD, reducing the number of available patients for study. Despite this, we believe that the insights gained from our study contribute meaningfully to the understanding of this under-researched disease. We also acknowledge that out of the 20 randomly chosen miRNAs to be validated by qPCR, only 11 were successfully validated due to technical constraints, including issues with qPCR primer design and the limited expression levels of some miRNAs. Furthermore, our study uses cross-sectional data, which restricts our ability to evaluate changes in miRNA expression over time. Longitudinal studies would be valuable in addressing this gap, allowing for the assessment of temporal changes in miRNA expression. Future research incorporating longitudinal data is needed to understand temporal dynamics and their implications for disease management. Further studies in other chronic liver diseases can also be performed to evaluate the specificity of miRNAs for liver injuries.

Acknowledgments

We would like to thank Ashish Sharma, Shannon Holiday, and Asha Rani for their advice and suggestions on this work, as well as members of our laboratories for their contributions to various aspects of our research. The ultrastructural studies were conducted at the University of Florida College of Medicine Electron Microscopy Core Facility under the kind supervision of Dr. Jill Verlander, with the assistance of Dr. Sharon Matthews. Small RNA sequencing and data analysis were performed at the Interdisciplinary Center for Biotechnology Research in the University of Florida's premier core research facility under the supervision of Drs. Yanping Zhang and Tongjun Gu.

Funding

This work was supported by a grant from the Alpha One Foundation (AGR00019116). Dr. Zhou is the recipient of a Research Career Scientist Award from the Department of Veterans Affairs (IK6BX004477).

Conflict of interest

The authors have no conflict of interests related to this publication.

Author contributions

Acquisition of data, technical support, review & editing (RO), data curation, formal analysis, review & editing (ZH), formal analysis, review & editing (ZG), formal analysis, review & editing (SD), acquisition of data (VC), formal analysis, review & editing (HZ), acquisition of data (JW), writing, review & editing (MH), conceptualization, supervision (MB), conceptualization, funding acquisition, formal analysis, data curation, supervision, writing the original draft, and review & editing (NK). All authors have approved the final version and publication of the manuscript.

Ethical statement

The study protocol was approved by the Clinical Research Ethics Committee of the University of Florida (IRB202101148), and written informed consent was obtained from all subjects in accordance with the Declaration of Helsinki Principles.

Data sharing statement

Data and code used to generate the miRNA-seq associated plots are hosted at the following repository: <https://github.com/zfg2013/EV-miRNA-and-AATD/tree/update>. All correspondence regarding the data & code used should be sent to Nazli Khodayari (nazli.khodayari@medicine.ufl.edu) or Zachary Greenberg (zfg2013@ufl.edu).

References

- [1] Janciauskiene SM, Bals R, Koczulla R, Vogelmeier C, Köhnlein T, Welte T. The discovery of α 1-antitrypsin and its role in health and disease. *Respir Med* 2011;105(8):1129–1139. doi:10.1016/j.rmed.2011.02.002, PMID:21367592.
- [2] Lindblad D, Blomenkamp K, Teckman J. Alpha-1-antitrypsin mutant Z protein content in individual hepatocytes correlates with cell death in a mouse model. *Hepatology* 2007;46(4):1228–1235. doi:10.1002/hep.21822, PMID:17886264.
- [3] Khodayari N, Oshins R, Holliday LS, Clark V, Xiao Q, Marek G, *et al*. Alpha-1 antitrypsin deficient individuals have circulating extracellular vesicles with profibrogenic cargo. *Cell Commun Signal* 2020;18(1):140. doi:10.1186/s12964-020-00648-0, PMID:32887613.
- [4] Perlmutter DH. Current and Emerging Treatments for Alpha-1 Antitrypsin

- Deficiency. *Gastroenterol Hepatol (N Y)* 2016;12(7):446–448. PMID:27489528.
- [5] Zamora MR, Ataya A. Lung and liver transplantation in patients with alpha-1 antitrypsin deficiency. *Ther Adv Chronic Dis* 2021;12:65–76. doi:10.1177/20406223211002988, PMID:34408830.
- [6] Sun M, Kisseleva T. Reversibility of liver fibrosis. *Clin Res Hepatol Gastroenterol* 2015;39(Suppl 1):S60–S63. doi:10.1016/j.clinre.2015.06.015, PMID:26206574.
- [7] Clark VC, Marek G, Liu C, Collinsworth A, Shuster J, Kurtz T, *et al*. Clinical and histologic features of adults with alpha-1 antitrypsin deficiency in a non-cirrhotic cohort. *J Hepatol* 2018;69(6):1357–1364. doi:10.1016/j.jhep.2018.08.005, PMID:30138687.
- [8] Abdi W, Millan JC, Mezey E. Sampling variability on percutaneous liver biopsy. *Arch Intern Med* 1979;139(6):667–669. PMID:443970.
- [9] Sung S, Kim J, Jung Y. Liver-Derived Exosomes and Their Implications in Liver Pathobiology. *Int J Mol Sci* 2018;19(12):3715. doi:10.3390/ijms19123715, PMID:30469540.
- [10] Cortez MA, Bueso-Ramos C, Ferdin J, Lopez-Berestein G, Sood AK, Calin GA. MicroRNAs in body fluids—the mix of hormones and biomarkers. *Nat Rev Clin Oncol* 2011;8(8):467–477. doi:10.1038/nrclinonc.2011.76, PMID:21647195.
- [11] Bandopadhyay M, Bharadwaj M. Exosomal miRNAs in hepatitis B virus related liver disease: a new hope for biomarker. *Gut Pathog* 2020;12:23. doi:10.1186/s13099-020-00353-w, PMID:32346400.
- [12] Chang Y, Han JA, Kang SM, Jeong SW, Ryu T, Park HS, *et al*. Clinical impact of serum exosomal microRNA in liver fibrosis. *PLoS One* 2021;16(9):e0255672. doi:10.1371/journal.pone.0255672, PMID:34506494.
- [13] Xu D, Di K, Fan B, Wu J, Gu X, Sun Y, *et al*. MicroRNAs in extracellular vesicles: Sorting mechanisms, diagnostic value, isolation, and detection technology. *Front Bioeng Biotechnol* 2022;10:948959. doi:10.3389/fbioe.2022.948959, PMID:36324901.
- [14] Lynøe N, Sandlund M, Dahlqvist G, Jacobsson L. Informed consent: study of quality of information given to participants in a clinical trial. *BMJ* 1991;303(6803):610–613. doi:10.1136/bmj.303.6803.610, PMID:1932901.
- [15] Brantly ML, Wittes JT, Vogelmeier CF, Hubbard RC, Fells GA, Crystal RG. Use of a highly purified alpha 1-antitrypsin standard to establish ranges for the common normal and deficient alpha 1-antitrypsin phenotypes. *Chest* 1991;100(3):703–708. doi:10.1378/chest.100.3.703, PMID:1889260.
- [16] Théry C, Witwer KW, Aikawa E, Alcaraz MJ, Anderson JD, Andriantsitohaina R, *et al*. Minimal information for studies of extracellular vesicles 2018 (MISEV2018): a position statement of the International Society for Extracellular Vesicles and update of the MISEV2014 guidelines. *J Extracell Vesicles* 2018;7(1):1535750. doi:10.1080/20013078.2018.1535750, PMID:30637094.
- [17] Kechin A, Boyarskikh U, Kel A, Filipenko M. cutPrimers: A New Tool for Accurate Cutting of Primers from Reads of Targeted Next Generation Sequencing. *J Comput Biol* 2017;24(11):1138–1143. doi:10.1089/cmb.2017.0096, PMID:28715235.
- [18] Langdon WB. Performance of genetic programming optimised Bowtie2 on genome comparison and analytic testing (GCAT) benchmarks. *BioData Min* 2015;8(1):1. doi:10.1186/s13040-014-0034-0, PMID:25621011.
- [19] Langmead B, Salzberg SL. Fast gapped-read alignment with Bowtie 2. *Nat Methods* 2012;9(4):357–359. doi:10.1038/nmeth.1923, PMID:22388286.
- [20] Anders S, Pyl PT, Huber W. HTSeq—a Python framework to work with high-throughput sequencing data. *Bioinformatics* 2015;31(2):166–169. doi:10.1093/bioinformatics/btu638, PMID:25260700.
- [21] Kozomara A, Griffiths-Jones S. miRBase: annotating high confidence microRNAs using deep sequencing data. *Nucleic Acids Res* 2014;42(Database issue):D68–D73. doi:10.1093/nar/gkt1181, PMID:24275495.
- [22] Bolger AM, Lohse M, Usadel B. Trimmomatic: a flexible trimmer for Illumina sequence data. *Bioinformatics* 2014;30(15):2114–2120. doi:10.1093/bioinformatics/btu170, PMID:24695404.
- [23] Phan L, Hsu J, Tri LQ, Willi M, Mansour T, Kai Y, *et al*. dbVar structural variant cluster set for data analysis and variant comparison. *F1000Res* 2016;5:673. doi:10.12688/f1000research.8290.2, PMID:28357035.
- [24] Li B, Dewey CN. RSEM: accurate transcript quantification from RNA-Seq data with or without a reference genome. *BMC Bioinformatics* 2011;12:323. doi:10.1186/1471-2105-12-323, PMID:21816040.
- [25] Khodayari N, Oshins R, Aranyos AM, Duarte S, Mostofizadeh S, Lu Y, *et al*. Characterization of hepatic inflammatory changes in a C57BL/6J mouse model of alpha1-antitrypsin deficiency. *Am J Physiol Gastrointest Liver Physiol* 2022;323(6):G594–G608. doi:10.1152/ajpgi.00207.2022, PMID:36256438.
- [26] Chen XM. MicroRNA signatures in liver diseases. *World J Gastroenterol* 2009;15(14):1665–1672. doi:10.3748/wjg.15.1665, PMID:19360909.
- [27] Robinson MD, McCarthy DJ, Smyth GK. edgeR: a Bioconductor package for differential expression analysis of digital gene expression data. *Bioinformatics* 2010;26(1):139–140. doi:10.1093/bioinformatics/btp616, PMID:19910308.
- [28] Robinson MD, Oshlack A. A scaling normalization method for differential expression analysis of RNA-seq data. *Genome Biol* 2010;11(3):R25. doi:10.1186/gb-2010-11-3-r25, PMID:20196867.
- [29] Damanti CC, Gaffo E, Lovisa F, Garbin A, Di Battista P, Galligani I, *et al*. MIR-26a-5p as a Reference to Normalize MicroRNA qRT-PCR Levels in Plasma Exosomes of Pediatric Hematological Malignancies. *Cells* 2021;10(1):101. doi:10.3390/cells10010101, PMID:33429910.
- [30] Zhang Y, Han T, Feng D, Li J, Wu M, Peng X, *et al*. Screening of non-invasive miRNA biomarker candidates for metastasis of gastric cancer by small RNA sequencing of plasma exosomes. *Carcinogenesis* 2020;41(5):582–590. doi:10.1093/carcin/bgz186, PMID:31740975.

- [31] Matsuura K, Aizawa N, Enomoto H, Nishiguchi S, Toyoda H, Kumada T, *et al*. Circulating let-7 Levels in Serum Correlate With the Severity of Hepatic Fibrosis in Chronic Hepatitis C. *Open Forum Infect Dis* 2018;5(11):ofy268. doi:10.1093/ofid/ofy268, PMID:30443558.
- [32] Matsuura K, De Giorgi V, Schechterly C, Wang RY, Farci P, Tanaka Y, *et al*. Circulating let-7 levels in plasma and extracellular vesicles correlate with hepatic fibrosis progression in chronic hepatitis C. *Hepatology* 2016;64(3):732–745. doi:10.1002/hep.28660, PMID:27227815.
- [33] Aly DM, Gohar NA, Abd El-Hady AA, Khairy M, Abdullatif MM. Serum microRNA let-7a-1/let-7d/let-7f and miRNA 143/145 Gene Expression Profiles as Potential Biomarkers in HCV Induced Hepatocellular Carcinoma. *Asian Pac J Cancer Prev* 2020;21(2):555–562. doi:10.31557/APJCP.2020.21.2.555, PMID:32102538.
- [34] Umezu T, Tsuneyama K, Kanekura K, Hayakawa M, Tanahashi T, Kawano M, *et al*. Comprehensive analysis of liver and blood miRNA in precancerous conditions. *Sci Rep* 2020;10(1):21766. doi:10.1038/s41598-020-78500-1, PMID:33303811.
- [35] Chen Y, Chen J, Liu Y, Li S, Huang P. Plasma miR-15b-5p, miR-338-5p, and miR-764 as Biomarkers for Hepatocellular Carcinoma. *Med Sci Monit* 2015;21:1864–1871. doi:10.12659/MSM.893082, PMID:26119771.
- [36] Dong Y, Zhang N, Zhao S, Chen X, Li F, Tao X. miR-221-3p and miR-15b-5p promote cell proliferation and invasion by targeting Axin2 in liver cancer. *Oncol Lett* 2019;18(6):6491–6500. doi:10.3892/ol.2019.11056, PMID:31814849.
- [37] Cisiotto J, do Amaral AE, Rosolen D, Rode MP, Silva AH, Winter E, *et al*. MicroRNA profiles in serum samples from Acute-On-Chronic Liver Failure patients and miR-25-3p as a potential biomarker for survival prediction. *Sci Rep* 2020;10(1):100. doi:10.1038/s41598-019-56630-5, PMID:31919459.
- [38] Zhang R, Zhang LJ, Yang ML, Huang LS, Chen G, Feng ZB. Potential role of microRNA-223-3p in the tumorigenesis of hepatocellular carcinoma: A comprehensive study based on data mining and bioinformatics. *Mol Med Rep* 2018;17(2):2211–2228. doi:10.3892/mmr.2017.8167, PMID:29207133.
- [39] Mehta R, Otgonsuren M, Younoszai Z, Allawi H, Raybuck B, Younossi Z. Circulating miRNA in patients with non-alcoholic fatty liver disease and coronary artery disease. *BMJ Open Gastroenterol* 2016;3(1):e000096. doi:10.1136/bmjgast-2016-000096, PMID:27493762.
- [40] Li L, Zhang X, Ren H, Huang X, Shen T, Tang W, *et al*. miR-23a/b-3p promotes hepatic lipid accumulation by regulating Srebp-1c and Fas. *J Mol Endocrinol* 2021;68(1):35–49. doi:10.1530/JME-20-0324, PMID:34723832.
- [41] Bian H, Zhou Y, Zhou D, Zhang Y, Shang D, Qi J. The latest progress on miR-374 and its functional implications in physiological and pathological processes. *J Cell Mol Med* 2019;23(5):3063–3076. doi:10.1111/jcmm.14219, PMID:30772950.
- [42] Ding W, Xin J, Jiang L, Zhou Q, Wu T, Shi D, *et al*. Characterisation of peripheral blood mononuclear cell microRNA in hepatitis B-related acute-on-chronic liver failure. *Sci Rep* 2015;5:13098. doi:10.1038/srep13098, PMID:26267843.
- [43] Mateescu B, Kowal EJ, van Balkom BW, Bartel S, Bhattacharyya SN, Buzás EI, *et al*. Obstacles and opportunities in the functional analysis of extracellular vesicle RNA – an ISEV position paper. *J Extracell Vesicles* 2017;6(1):1286095. doi:10.1080/20013078.2017.1286095, PMID:28326170.
- [44] Wen Y, Han J, Chen J, Dong J, Xia Y, Liu J, *et al*. Plasma miRNAs as early biomarkers for detecting hepatocellular carcinoma. *Int J Cancer* 2015;137(7):1679–1690. doi:10.1002/ijc.29544, PMID:25845839.
- [45] Gharib AF, Eed EM, Khalifa AS, Raafat N, Shehab-Eldeen S, Alwakeel HR, *et al*. Value of Serum miRNA-96-5p and miRNA-99a-5p as Diagnostic Biomarkers for Hepatocellular Carcinoma. *Int J Gen Med* 2022;15:2427–2436. doi:10.2147/IJGM.S354842, PMID:35264879.
- [46] Guo Y, Xiong Y, Sheng Q, Zhao S, Wattacheril J, Flynn CR. A micro-RNA expression signature for human NAFLD progression. *J Gastroenterol* 2016;51(10):1022–1030. doi:10.1007/s00535-016-1178-0, PMID:26874844.
- [47] Liu YM, Ma JH, Zeng QL, Lv J, Xie XH, Pan YJ, *et al*. MiR-19a Affects Hepatocyte Autophagy via Regulating lncRNA NBR2 and AMPK/PPARα in D-GalN/Lipopolysaccharide-Stimulated Hepatocytes. *J Cell Biochem* 2018;119(1):358–365. doi:10.1002/jcb.26188, PMID:28586153.
- [48] Yao X, Zhang H, Liu Y, Liu X, Wang X, Sun X, *et al*. miR-99b-3p promotes hepatocellular carcinoma metastasis and proliferation by targeting protocadherin 19. *Gene* 2019;698:141–149. doi:10.1016/j.gene.2019.02.071, PMID:30849536.
- [49] Li WF, Dai H, Ou Q, Zuo GQ, Liu CA. Overexpression of microRNA-30a-5p inhibits liver cancer cell proliferation and induces apoptosis by targeting MTDH/PTEN/AKT pathway. *Tumour Biol* 2016;37(5):5885–5895. doi:10.1007/s13277-015-4456-1, PMID:26589417.
- [50] Cheng B, Ding F, Huang CY, Xiao H, Fei FY, Li J. Role of miR-16-5p in the proliferation and metastasis of hepatocellular carcinoma. *Eur Rev Med Pharmacol Sci* 2019;23(1):137–145. doi:10.26355/eurrev_201901_16757, PMID:30657555.
- [51] Wang C, Wang X, Su Z, Fei H, Liu X, Pan Q. MiR-25 promotes hepatocellular carcinoma cell growth, migration and invasion by inhibiting RhoGDI1. *Oncotarget* 2015;6(34):36231–36244. doi:10.18632/oncotarget.4740, PMID:26460549.
- [52] Messner CJ, Schmidt S, Özkul D, Gaiser C, Terracciano L, Krähenbühl S, *et al*. Identification of miR-199a-5p, miR-214-3p and miR-99b-5p as Fibrosis-Specific Extracellular Biomarkers and Promoters of HSC Activation. *Int J Mol Sci* 2021;22(18):9799. doi:10.3390/ijms22189799, PMID:34575957.
- [53] Jiang XP, Ai WB, Wan LY, Zhang YQ, Wu JF. The roles of microRNA families in hepatic fibrosis. *Cell Biosci* 2017;7:34. doi:10.1186/s13578-017-0161-7, PMID:28680559.
- [54] Dunham RM, Thapa M, Velazquez VM, Elrod EJ, Denning TL, Pulendran B, *et al*. Hepatic stellate cells preferentially induce Foxp3+ regulatory T cells by production of retinoic acid. *J Immunol* 2013;190(5):2009–2016. doi:10.4049/jimmunol.1201937, PMID:23359509.
- [55] Song LY, Ma YT, Wu CF, Wang CJ, Fang WJ, Liu SK. MicroRNA-195 Activates Hepatic Stellate Cells In Vitro by Targeting Smad7. *Biomed Res Int* 2017;2017:1945631. doi:10.1155/2017/1945631, PMID:28929107.
- [56] Zhang B, Wu F, Li P, Li H. ARRDC3 inhibits liver fibrosis and epithelial-to-mesenchymal transition via the ITGB4/PI3K/Akt signaling pathway. *Immunopharmacol Immunotoxicol* 2023;45(2):160–171. doi:10.1080/08923973.2022.2128369, PMID:36154540.
- [57] Zhang Y, Guo J, Li Y, Jiao K, Zhang Y. let-7a suppresses liver fibrosis via TGFβ/SMAD signaling transduction pathway. *Exp Ther Med* 2019;17(5):3935–3942. doi:10.3892/etm.2019.7457, PMID:31007736.
- [58] Liu J, Fan L, Yu H, Zhang J, He Y, Feng D, *et al*. Endoplasmic Reticulum Stress Causes Liver Cancer Cells to Release Exosomal miR-23a-3p and Up-regulate Programmed Death Ligand 1 Expression in Macrophages. *Hepatology* 2019;70(1):241–258. doi:10.1002/hep.30607, PMID:30854665.
- [59] Khodayari N, Wang RL, Oshins R, Lu Y, Millett M, Aranyos AM, *et al*. The Mechanism of Mitochondrial Injury in Alpha-1 Antitrypsin Deficiency Mediated Liver Disease. *Int J Mol Sci* 2021;22(24):13255. doi:10.3390/ijms222413255, PMID:34948056.
- [60] Sun LY, Wang N, Ban T, Sun YH, Han Y, Sun LL, *et al*. MicroRNA-23a mediates mitochondrial compromise in estrogen deficiency-induced concentric remodeling via targeting PGC-1α. *J Mol Cell Cardiol* 2014;75:1–11. doi:10.1016/j.yjmcc.2014.06.012, PMID:24984145.